

Dont fall into the gap: GW190521 as a straddling binary

Maya Fishbach*

*Department of Astronomy and Astrophysics, University of Chicago, Chicago, IL 60637, USA
Center for Interdisciplinary Exploration and Research in Astrophysics (CIERA) and Department of Physics and Astronomy,
Northwestern University, 1800 Sherman Ave, Evanston, IL 60201, USA*

Daniel E. Holz

*Enrico Fermi Institute, Department of Physics, Department of Astronomy and Astrophysics,
and Kavli Institute for Cosmological Physics, University of Chicago, Chicago, IL 60637, USA*

Models for black hole (BH) formation from stellar collapse robustly predict the existence of a pair-instability supernova (PISN) mass gap: black holes *cannot* be born with masses in the range $50 M_{\odot} \lesssim m \lesssim 120 M_{\odot}$. The reported mass of GW190521’s primary black hole, $m_1 = 85_{-14}^{+21} M_{\odot}$, falls squarely within this PISN mass gap. Moreover, under the same uninformative priors used for m_1 , GW190521’s secondary black hole is also likely in the PISN mass gap ($m_2 > 50 M_{\odot}$ at 93% confidence). Even in proposed scenarios which can produce BHs in the mass gap, *double* mass-gap binary black holes (BBHs) are expected to be rare. We consider the more conservative alternative that GW190521’s secondary BH belongs to the population of BHs previously observed by LIGO/Virgo, finding $m_2 < 48 M_{\odot}$ at 90% credibility. With this prior on m_2 , we automatically find that the mass of the primary BH has a 39% probability of being *above* the gap ($m_1 > 120 M_{\odot}$, or 25% probability for $m_1 > 130 M_{\odot}$). This is because the total mass of the system is better constrained than the individual masses, so as the secondary mass drops to lower values, the primary mass increases to higher values. As long as the prior odds for a double-mass-gap BBH are smaller than $\sim 1 : 15$, it is more likely that GW190521 straddles the pair-instability gap. Alternatively, if we assume a gap width of $\gtrsim 75 M_{\odot}$ as predicted from stellar evolution, and assume that both components of GW190521 are formed from stellar collapse, we again find that GW190521’s BHs straddle the mass gap, with the upper edge of the gap above $116 M_{\odot}$ (90% credibility). We argue that GW190521 may not present a fundamental challenge to our understanding of stellar evolution and collapse. Instead, GW190521 may be the first example of a straddling binary black hole, composed of a conventional stellar mass BH and a BH from the “far side” of the PISN mass gap.

I. INTRODUCTION

GW190521 is one of the most surprising and exciting systems detected thus far by the LIGO [1] and Virgo [2] gravitational-wave detector network. This system was detected at high confidence, with a false alarm rate of $< 1/4900$ years [3]. Parameter estimation constrains the total mass of the system to be $150_{-17}^{+29} M_{\odot}$, with a primary mass of $85_{-14}^{+21} M_{\odot}$ and a secondary mass of $66_{-18}^{+17} M_{\odot}$ [3, 4].

Meanwhile, stellar physics predicts the existence of a BH mass gap, with no BHs in the mass range $50 M_{\odot} \lesssim m \lesssim 120 M_{\odot}$ due to (pulsational) pair-instability supernovae [5–12]. While standard uncertainties on nuclear reaction rates [13, 14], super-Eddington accretion [15], convection [16], and rotation [17] may raise the lower edge of the gap by a few solar masses, the lower edge of the gap cannot extend past $65 M_{\odot}$ [18–21] without invoking new physics [22, 23]. Above the gap, stars of sufficiently high mass avoid pair-instability, and are expected to collapse into BHs with masses above ~ 120 – $135 M_{\odot}$ [18, 24, 25].

On the observational side, BBH observations in the first two observing runs of LIGO/Virgo have already placed constraints on the location of the mass gap [26–

28]. If the lower-edge of the mass gap is sharp, it is observationally measured to be $m_{\max} = 40.8_{-4.4}^{+11.8} M_{\odot}$ (90% credibility) using the LIGO/Virgo GWTC-1 observations [27, 29], or $41_{-5}^{+10} M_{\odot}$ when including the IAS catalogs [28]. It is to be noted that LIGO and Virgo are also sensitive to black holes with masses above the gap, and are beginning to constrain the rate of such mergers [30, 31]. These “far side” black holes leave an imprint on the stochastic background of unresolved binaries, would provide unique standard siren constraints on the cosmic expansion at redshift $z \sim 1$, and may also be observable by *LISA* [32].

At first glance, the primary mass of GW190521 falls squarely within this mass gap, having only 0.3% probability of being below $65 M_{\odot}$ [3]. Several scenarios, including hierarchical mergers of smaller BHs in stellar clusters or AGN disks [33–38], primordial BHs [39], and stellar mergers [40, 41] may produce BHs in the mass gap; a detailed discussion of the various possibilities is found in Abbott *et al.* [4]. The hierarchical merger scenario is of particular interest when one notes that the merger remnant of GW170729 [29] was a BH of mass $80.3_{-10.2}^{+14.6} M_{\odot}$, and so LIGO/Virgo have already witnessed the creation of a BH which is consistent with the reported mass of GW190521’s primary.

However, even in these scenarios, the merger rate of systems involving a mass gap BH is expected to be low—more than two orders of magnitude smaller than the

* NASA Einstein Fellow; maya.fishbach@northwestern.edu

merger rate between non-mass gap BHs [40, 42–44], especially when compared to the merger rate inferred by LIGO/Virgo [27, 29]. The merger rate of systems involving *two* mass gap BHs is expected to be even smaller by orders of magnitude. Recently Kimball *et al.* [45] analyzed the GWTC-1 observations under a phenomenological framework tuned to globular cluster simulations, finding that, compared to first-generation BHs, the relative rate of mergers involving one second-generation BH is $\sim 2.5 \times 10^{-3}$, and the relative rate of mergers involving two second-generation BHs is $\sim 3.1 \times 10^{-6}$.

Because of these low expected rates, following the method of Kimball *et al.* [45], Abbott *et al.* [4] found that a hierarchical-merger origin for GW190521 is modestly disfavored by the data by factors of ~ 1.1 –5, depending on the choice of gravitational waveform model used for parameter estimation. Abbott *et al.* [4] also noted that there is some probability that m_1 is a first-generation BH with primary mass above the PISN gap. However, they concluded that including this possibility in the model for the first-generation mass distribution would not significantly alter their results for the relative probabilities of first-generation to second-generation mergers. Even without this possibility, the analysis of Abbott *et al.* [4] finds that both components of GW190521 are likely to be first-generation BHs.

In this paper, we build on the idea that GW190521 contains at least one conventional, first-generation BH. In Section II, we reanalyze the data with the assumption that the secondary BH is a member of the BH mass distribution inferred from LIGO/Virgo’s first two observing runs, characterized by a maximum mass at $m_{\text{max}} = 40.8^{+11.8}_{-4.4} M_{\odot}$ [27] with the population tapering off above this. We find $m_2 < 48 M_{\odot}$ at 90% credibility. Because the total mass of GW190521 is constrained to be $M = 150^{+29}_{-17} M_{\odot}$, the updated inference on m_2 in turn implies that m_1 is likely to be on the far side of the gap: $m_1 = 113^{+33}_{-24} M_{\odot}$ (90% credibility), with a 39% chance that $m_1 > 120 M_{\odot}$. Therefore, under the assumption that the secondary BH is conventional, the primary BH of GW190521 is likely to be the first intermediate mass black hole (IMBH) detected by LIGO/Virgo; $m_1 > 100 M_{\odot}$ at 81% credibility. Similarly, we reanalyze GW190521 with the assumption of a PISN gap of fixed width greater than $75 M_{\odot}$, and find that, if both component BHs avoid the gap, this naturally constrains the upper edge of the gap to be above $116 M_{\odot}$ (90% credibility). We conclude in Section III. The Appendix contains a calculation of the Bayes factors between the different priors considered, which support the interpretation that GW190521 straddles the mass gap.

II. METHODS AND RESULTS

The analysis of GW190521’s component masses presented in Abbott *et al.* [3, 4] utilized uninformative priors. In particular, their analysis presumes that the distribu-

tion of BH masses is uniform in detector-frame component masses $m_1(1+z)$ and $m_2(1+z)$, and uniform in luminosity-distance-volume (i.e., $p(d_L) \propto d_L^2$). The chosen prior ranges are such that the likelihood is contained entirely within the prior bounds. Abbott *et al.* [4] infers the posterior distribution under these priors, using three different waveform choices: NRSurd7q4 [46], IMRPhenomPv3HM [47–52], and SEOBNRv4PHM [53–55]. We show the m_1 posterior from this analysis, using the NRSurd7q4 waveform, as the dashed curve in the left panel of Fig. 1.

For the remainder of this work, we reweight the posterior samples from Abbott *et al.* [4] to a slightly different choice of uninformative prior. Instead of uniform in detector-frame component masses, we pick uniform in source-frame component masses, and instead of uniform in d_L^3 , we take uniform in comoving volume and source-frame time, $p(z) \propto dV_c/dz(1+z)^{-1}$ (see Eq. C1 in Ref. [27]). The posterior on m_1 under this slightly modified prior is shown as the solid curves in the left panel of Fig. 1; this new uninformative prior implies a slight shift in the source-frame m_1 compared to the prior of Abbott *et al.* [4]. The joint posterior over m_1 and m_2 under this new uninformative prior is shown as the purple contours of Fig. 2. Because our uninformative prior is flat over source-frame m_1 and m_2 , comoving volume, and source-frame time, the resulting posterior over these parameters is proportional to the marginal likelihood.

Under this uninformative prior, the probability that $m_1 > 120 M_{\odot}$ is 1.7% for the “preferred” NRSurd7q4 waveform model, and $< 0.002\%$ for $m_1 < 45 M_{\odot}$. The posterior under the uninformative prior therefore favors that m_1 sits squarely in the mass gap. Moreover, under this prior, $m_2 > 45 M_{\odot}$ at 97.4% credibility, which would place m_2 in the mass gap as well. Theoretical predictions disfavor double-mass-gap systems by a factor of $\gtrsim 1000$, making it reasonable to consider an alternative, population-informed prior on m_2 . In fact, we find that the Bayes factor between the flat (m_1, m_2) prior and this alternative prior is only ~ 7 (see the Appendix), which is easily overcome by the prior odds disfavoring double-mass-gap systems. In the following we explore how imposing a population-informed prior on the secondary mass affects not only the m_2 posterior, but also the primary mass posterior of GW190521.

Combining multiple events in a population analysis allows us to update our inference on the parameters of the individual events. By learning the population distribution, a hierarchical Bayesian framework updates the prior distribution of the individual-event parameters [56–59]. In other words, a population analysis self-consistently infers the shape of the population distribution (i.e., the mass and spin distributions) jointly with the parameters of individual events. Doctor *et al.* [60] and Kimball *et al.* [45] recently developed and performed such population analyses explicitly designed to accommodate a potential BBH subpopulation within the mass gap, allowing for the possibility that these systems form via hierarchical merg-

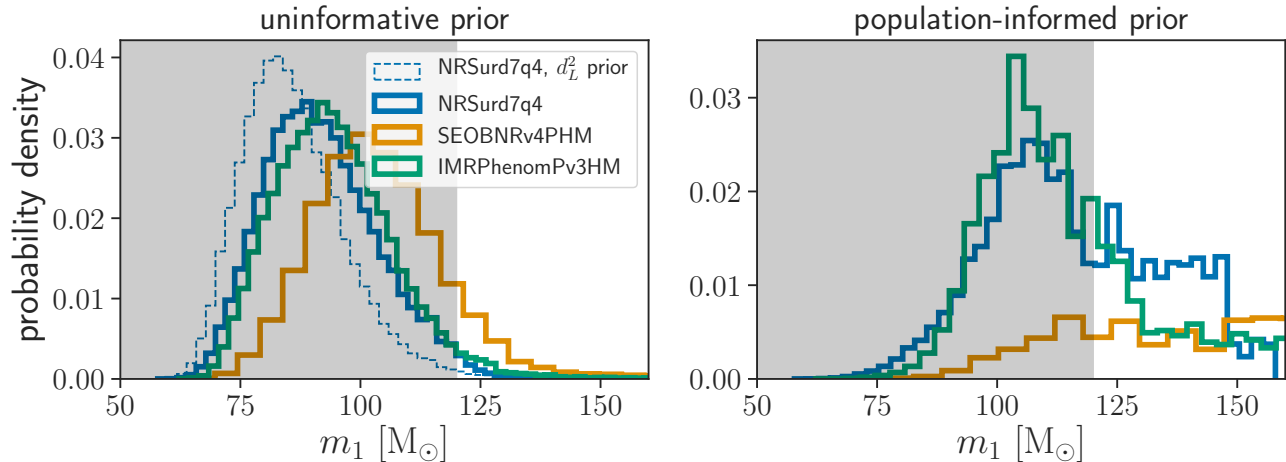


FIG. 1. Posterior distribution on the source-frame primary mass using an *uninformative* prior (left), compared to a population-informed prior (right) that assumes that m_2 belongs to the population of first-generation black holes inferred from LIGO/Virgo’s catalog GWTC-1 [27]. The different colored histograms show the results under the different waveform models in Abbott *et al.* [3, 4]. On the left, the distributions assume a flat prior on m_1 and m_2 and a flat prior on the comoving spacetime volume (the dashed blue histogram shows the posterior under the “default” flat-in-detector-frame masses and $p(d_L) \propto d_L^2$ luminosity distance prior presented in Abbott *et al.* [3, 4]). On the right, we impose a prior on m_2 according to the component mass distribution inferred from the GWTC-1 distribution [27], but leave the flat prior on m_1 (note that the new prior is on m_2 , but we are plotting m_1). The shaded band denotes the region of the posterior with $m_1 < 120 M_\odot$, in which m_1 would be in the PISN mass gap. Under the uninformative prior, the probability that $m_1 > 120 M_\odot$ is 1.7%, 3.3%, and 14% for the NRSurd7q4, IMRPhenomPv3HM, and SEOBNRv4PHM waveform models respectively. Under the assumption that m_2 belongs to the black hole population found in GWTC-1, the probabilities for $m_1 > 120 M_\odot$ increase to 39%, 31%, and 89% under the respective waveform models.

ers of the below-mass-gap subpopulation [61, 62]. As discussed in Section I, Abbott *et al.* [4] applied the analysis proposed by Kimball *et al.* [45], analyzing GW190521 jointly with LIGO/Virgo’s ten BBH observations from the first two observing runs, GWTC-1 [29]. However, the BBH population inferred from GWTC-1 does not constrain the rate of mergers above the gap, and so these population analyses did not allow for the possibility of a first-generation BH beyond the PISN gap. Abbott *et al.* [4] noted that allowing for this possibility would not significantly affect the conclusions from the hierarchical merger analysis, which found that a first-generation origin for GW190521 is slightly preferred even without the additional probability of m_1 lying above the gap.

Under the assumption that BBH systems involving two mass-gap BHs are a few orders of magnitude more rare than systems involving just one mass-gap BH [43, 45], we explore the assumption that the secondary mass of GW190521 is a conventional BH belonging to the component BH population that LIGO/Virgo observed in their first two observing runs. Rather than performing a fully self-consistent population analysis that fits for both component masses of GW190521 together with previous BBH observations as in Doctor *et al.* [60] and Kimball *et al.* [45], we pursue a simpler, less rigorous approach. In this approach, we put a population prior only on the secondary mass of GW190521, assuming it is drawn from the

same population as the component masses of the BBH events observed in O1 and O2.

The mass distribution of BBHs inferred from the first two observing runs of LIGO/Virgo is presented in Abbott *et al.* [27], with a recent update incorporating IAS detections in Roulet *et al.* [28]. In particular, the one-dimensional mass distribution describing component BHs is found to be well-fit by a power law with a variable slope, minimum mass, and maximum mass cutoff; see for example Model B in Abbott *et al.* [27]. As has been emphasized [26–28], there is evidence for a sharp drop at $\sim 45 M_\odot$ in the mass spectrum of the component BHs found in BBH systems. The measurement of the maximum mass cutoff at $m_{\max} = 40.8^{+11.8}_{-4.4} M_\odot$ is consistent with expectations from PISN modeling.

Neglecting the mass ratio distribution for the moment, we can use the one-dimensional mass spectrum inferred under Model B in Abbott *et al.* [27] to construct a prior on the mass of a conventional BH (in other words, a BH that is drawn from this same population), marginalizing over the uncertainty in the population parameters. (See Fishbach and Holz [63] for a discussion of the sometimes subtle distinction between the component mass distribution, the primary mass distribution, and the secondary mass distribution.) This population-informed prior is given by the posterior population distribution (PPD) in-

ferred from Abbott *et al.* [27]:

$$p(m | d_{O1+O2}) \propto \int p(m | \theta) p(\theta | d_{O1+O2}) d\theta, \quad (1)$$

where $\theta = \{\alpha_m, \beta_q, m_{\min}, m_{\max}\}$ are the population hyperparameters of the power-law mass distribution model (Model B) and $p(\theta | d_{O1+O2})$ is the hyperposterior on these parameters inferred from the first two observing runs [27]. Although we use the above PPD as a prior for m_2 , we retain the uninformative, uniform prior on m_1 .

Applying the inferred PPD as a prior on the secondary mass of GW190521, while maintaining the flat prior on m_1 , significantly affects the m_2 posterior. Using uninformative priors, there is only a 2.6% probability that $m_2 < 45 M_\odot$, while this rises to 85% with the population-informed prior (NRSurd7q4 waveform). It would be unsurprising for a statistical fluctuation of this magnitude to affect the measured masses of GW190521; we expect that one out of ~ 40 events will have its true mass in the 2.5% tail of the likelihood.

Moreover, because the total mass of GW190521 is constrained to be $150_{-17}^{+29} M_\odot$, the updated m_2 posterior affects the joint posterior on m_1 and m_2 ; see Fig. 2. The implied marginal posterior on m_1 , under the informed prior on m_2 , is shown in the right panel of Fig. 1. We find that applying an astrophysical prior on m_2 results not only in m_2 dropping out of the mass gap to lower values, but also results in the m_1 posterior increasing to $113_{-24}^{+33} M_\odot$ and potentially crossing the upper edge of the PISN mass gap ($m_1 > 120 M_\odot$ with 39% credibility). Applying the GWTC-1 population priors on m_2 thus results in significant support for the two black hole masses straddling the PISN gap, with one below and one above. In the Appendix, we find that the likelihood ratio between a flat prior on (m_1, m_2) and a population-informed prior on m_2 coupled with a flat prior on $m_1 > 120 M_\odot$ is of order unity.

An alternative approach is to take a theoretically-motivated prior rather than a population prior determined by previous observations. Here, we take the width of the mass gap as fixed by theory, while allowing the placement of the upper and lower edges of the gap to be determined by the data. The width of the gap may face fewer theoretical uncertainties than the precise location of the edges of the gap; Farmer *et al.* [14] predict a width of $83_{-8}^{+5} M_\odot$. We re-analyze GW190521 assuming that neither BH sits in the mass gap, with a mass gap of $> 75 M_\odot$ as our prior. In particular, as discussed above, there is more likelihood support for m_1 being above the mass gap rather than below (by a factor of $\gtrsim 20$), and similarly there is significantly more support for m_2 being below the mass gap rather than above (by a factor of $\gtrsim 2 \times 10^5$). Enforcing $m_1 - m_2 > 75 M_\odot$ while using a uniform prior on the values of the individual masses, we find $m_1 > 116 M_\odot$ (90% posterior probability) and $m_2 < 41 M_\odot$ (90% probability); the updated m_1 and m_2 posteriors are shown in Fig. 3. We also note that, as was the case in Fig. 2, the values of m_1 and m_2 are correlated.

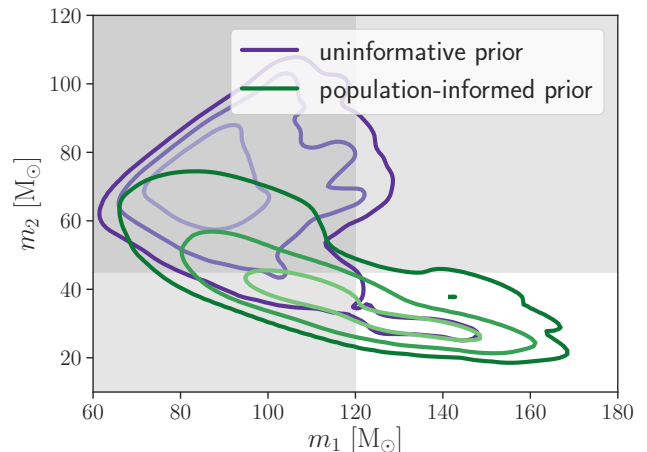


FIG. 2. Two-dimensional version of Fig. 1, showing results from the NRSurd7q4 waveform. Contours show 50%, 90%, and 99% credible regions. The shaded bands show $m_2 > 45 M_\odot$ (excluded if we believe that m_2 is a conventional BH) and $m_1 < 120 M_\odot$ (excluded if we believe that m_1 is a conventional BH). The unshaded region corresponds to the scenario in which the components straddle the gap. The other waveform models permit larger values of $m_1 - m_2$, thereby increasing the support for $m_1 > 120 M_\odot$ and $m_2 < 45 M_\odot$.

High values of m_1 , which push the BH up and out of the mass gap, are accompanied by lower values of m_2 which cause it to drop out of the mass gap.

As previously mentioned, the arguments laid out in this work are not rooted in a full population analysis, in contrast with the analysis of Kimball *et al.* [45] and Abbott *et al.* [4]. A careful population analysis would analyze all BBH events observed thus far simultaneously, including mass, spin and redshift information, and explicitly model the distribution of mergers above the gap, taking into account upper limits on the rate of such mergers from the first two observing runs [30]. Since we currently lack an observed population of BH events above the gap or theoretical guidance for the shape of the mass distribution at such high masses, we take a simple approach that applies a one-dimensional population prior to m_2 alone. Thus, we do not take into account prior knowledge regarding the relationship between the two component masses in a binary. We implicitly assume that a mass ratio $q < 0.5$ is as likely as a mass ratio of 1. While this is contrary to expectations from the first two observing runs, which favored equal-mass binaries [27, 28, 63, 64], we already know from the detection of GW190412 that asymmetric systems are not uncommon, with 10% of BBH systems likely having mass ratios more extreme than $q < 0.4$ [65]. We thus expect that under a full population analysis, the implied mass ratio of GW190521 under our proposed scenario ($q \sim 0.4$) would be reasonable. Even in the event that the underlying BBH population prefers near-unity mass ratios, and there

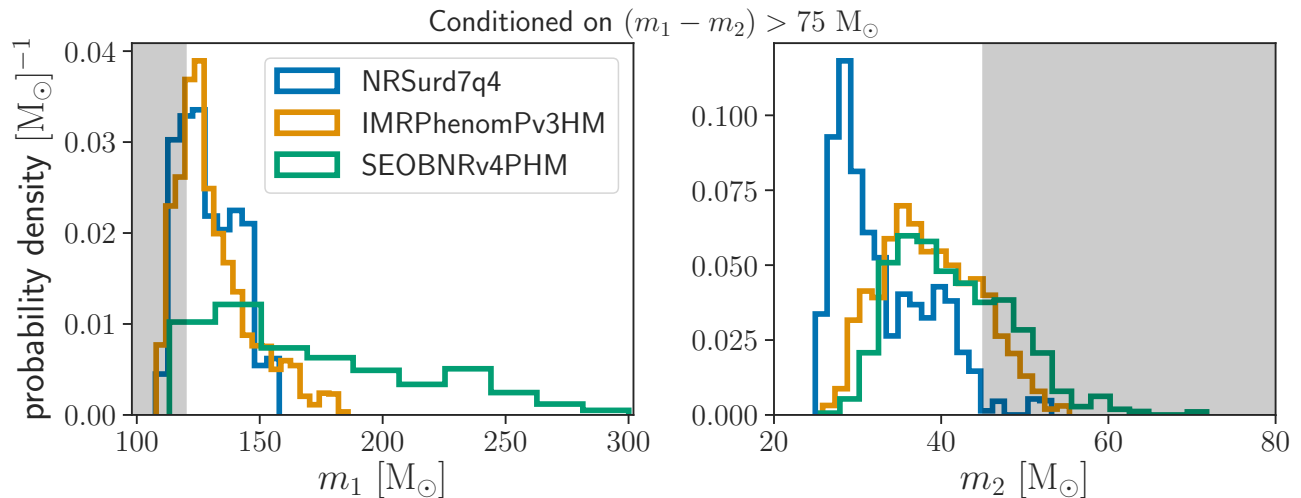


FIG. 3. Posterior distribution on the source-frame primary mass (left) and source-frame secondary mass (right), assuming that a mass gap of width $> 75 M_{\odot}$ [14] separates m_1 and m_2 . In this scenario, the primary mass lies above $116 M_{\odot}$ (90% credibility; NRSurd7q4 waveform model), which can be interpreted as a lower limit on the upper edge of the pair-instability gap under this assumption. Meanwhile, the secondary mass lies below $41 M_{\odot}$ (90% credibility; NRSurd7q4 waveform model). The shaded bands show $m_1 < 120 M_{\odot}$ (left) and $m_2 > 45 M_{\odot}$ (right). Taking the width of the gap is a theoretical prior, the updated posteriors on m_1 and m_2 are consistent with theoretical predictions for the location of the gap edges.

exists a population of BHs above the gap, LIGO/Virgo at current sensitivities may be less likely to detect a $120\text{--}120 M_{\odot}$ merger at cosmological distances than a system with a lower total mass similar to GW190521, as the more massive merger will merge at low frequencies out of the detectors’ sensitive band [30, 31].

A future population analysis should also account for BH spins. BH spin magnitudes of ~ 0.7 are a signature of hierarchical mergers, and more generally dynamically-assembled binaries are expected to have an isotropic distribution of spin tilts. These signatures can be used to distinguish between formation channels [61, 62, 66–69]. In this analysis, we do not consider spin information. While GW190521 displays mild hints of spin precession, which may make it more consistent with a dynamical- and possibly hierarchical-merger origin, the preference for spin precession as measured by the χ_p parameter is inconclusive [3, 4]. The updated mass priors considered in this work do not significantly increase or decrease the mild preference seen for precession under the uninformative prior (for precession, $\chi_p > 0$, where $0 \leq \chi_p \leq 1$ by definition). The uninformative prior finds $\chi_p > 0.5$ at 79% credibility; our population prior on m_2 , which retains an uninformative spin prior, finds $\chi_p > 0.5$ at 77% credibility.

III. CONCLUSIONS

GW190521 is one of the most surprising and important BBH merger detections to date. When analyzed with uninformative priors, both component masses of GW190521

fall within the PISN mass gap. This implies either a breakdown of our basic understanding of stellar explosions, or the existence of novel processes such as hierarchical mergers of smaller black holes or stellar mergers. We emphasize that double mass-gap BBHs are expected to be exceedingly rare, accounting for at most 0.1% of the inferred LIGO/Virgo rate.

In this paper we have analyzed GW190521 with population-informed priors, under the assumption that a merger with at most one mass-gap BH is *a priori* more likely than a double mass-gap merger. We have used the existing population of BBH detections to set a mass prior on the secondary BH (which, although it falls predominantly in the gap, has non-zero support below the gap). With this prior applied only to the secondary, we naturally find that the primary black hole has significant support *above* the gap, making GW190521 the first observed merger between a stellar-mass BH and an IMBH. We also analyze GW190521 with an astrophysically-informed prior that there exists a gap of width $75 M_{\odot}$. In this case, we again find that GW190521 consists of a straddling binary, with component masses on either side of the gap. Such a straddling binary fits with stellar theory, and does not necessarily require more speculative or unusual formation channels.

GW190521 has demonstrated that there must either be a population of BBH systems with both components within the PISN gap, or a population of component BHs with masses above the gap. The interpretation of GW190521 as a double-mass-gap BBH or a straddling binary depends on the assumed priors. Taking the conservative assumption that at least one of the components

of GW190521 belongs to the already-observed population of BBH systems, we find that GW190521 is more likely to be a straddling binary. Future BBH observations will help resolve this question. While the measurement uncertainty on individual events is large and thus prior-dependent, a population of BBH systems will reveal the shape of the BBH mass distribution, allowing us to firmly measure the rate of double-mass-gap binaries compared to the rate of mergers with components above the gap.

ACKNOWLEDGMENTS

We thank Christopher Berry, Juan Calderon Bustillo, Michael Coughlin, Reed Essick, Vicky Kalogera, Ajit Mehta, Javier Roulet and members of the LIGO/Virgo collaboration for useful discussions. MF was supported

by the NSF Graduate Research Fellowship Program under grant DGE-1746045, and by NASA through the NASA Hubble Fellowship grant HST-HF2-51455.001-A awarded by the Space Telescope Science Institute. MF and DEH were supported by NSF grants PHY-1708081 and PHY-2011997, the Kavli Institute for Cosmological Physics at the University of Chicago and an endowment from the Kavli Foundation. DEH gratefully acknowledges a Marion and Stuart Rice Award. This research has made use of data, software and/or web tools obtained from the Gravitational Wave Open Science Center (<https://www.gw-openscience.org>), a service of LIGO Laboratory, the LIGO Scientific Collaboration and the Virgo Collaboration. LIGO is funded by the U.S. National Science Foundation. Virgo is funded by the French Centre National de Recherche Scientifique (CNRS), the Italian Istituto Nazionale della Fisica Nucleare (INFN) and the Dutch Nikhef, with contributions by Polish and Hungarian institutes.

-
- [1] J. Aasi *et al.*, CQGra **32**, 074001 (2015), arXiv:1411.4547 [gr-qc].
 - [2] F. Acernese *et al.*, CQGra **32**, 024001 (2015), arXiv:1408.3978 [gr-qc].
 - [3] R. Abbott *et al.* (LIGO Scientific Collaboration and Virgo Collaboration), PhRvL **125**, 101102 (2020).
 - [4] R. Abbott *et al.*, ApJL **900**, L13 (2020).
 - [5] W. A. Fowler and F. Hoyle, ApJS **9**, 201 (1964).
 - [6] Z. Barkat, G. Rakavy, and N. Sack, PhRvL **18**, 379 (1967).
 - [7] W. W. Ober, M. F. El Eid, and K. J. Fricke, A&A **119**, 61 (1983).
 - [8] J. R. Bond, W. D. Arnett, and B. J. Carr, ApJ **280**, 825 (1984).
 - [9] A. Heger, C. L. Fryer, S. E. Woosley, N. Langer, and D. H. Hartmann, ApJ **591**, 288 (2003), arXiv:astro-ph/0212469 [astro-ph].
 - [10] S. E. Woosley, S. Blinnikov, and A. Heger, Nature **450**, 390 (2007), arXiv:0710.3314 [astro-ph].
 - [11] K.-J. Chen, A. Heger, S. Woosley, A. Almgren, and D. J. Whalen, ApJ **792**, 44 (2014), arXiv:1402.5960 [astro-ph.HE].
 - [12] T. Yoshida, H. Umeda, K. Maeda, and T. Ishii, MNRAS **457**, 351 (2016), arXiv:1511.01695 [astro-ph.SR].
 - [13] R. Farmer, M. Renzo, S. E. de Mink, P. Marchant, and S. Justham, ApJ **887**, 53 (2019), arXiv:1910.12874 [astro-ph.SR].
 - [14] R. Farmer, M. Renzo, S. de Mink, M. Fishbach, and S. Justham, arXiv e-prints, arXiv:2006.06678 (2020), arXiv:2006.06678 [astro-ph.HE].
 - [15] L. A. C. van Son, S. E. De Mink, F. S. Broekgaarden, M. Renzo, S. Justham, E. Laplace, J. Morán-Fraile, D. D. Hendriks, and R. Farmer, ApJ **897**, 100 (2020), arXiv:2004.05187 [astro-ph.HE].
 - [16] M. Renzo, R. J. Farmer, S. Justham, S. E. de Mink, Y. Göteborg, and P. Marchant, MNRAS **493**, 4333 (2020), arXiv:2002.08200 [astro-ph.SR].
 - [17] P. Marchant and T. J. Moriya, A&A **640**, L18 (2020), arXiv:2007.06220 [astro-ph.HE].
 - [18] K. Belczynski, A. Heger, W. Gladysz, A. J. Ruiter, S. Woosley, G. Wiktorowicz, H. Y. Chen, T. Bulik, R. O’Shaughnessy, D. E. Holz, C. L. Fryer, and E. Berti, A&A **594**, A97 (2016), arXiv:1607.03116 [astro-ph.HE].
 - [19] M. Spera and M. Mapelli, MNRAS **470**, 4739 (2017), arXiv:1706.06109 [astro-ph.SR].
 - [20] S. Stevenson, M. Sampson, J. Powell, A. Vigna-Gómez, C. J. Neijssel, D. Szécsi, and I. Mandel, ApJ **882**, 121 (2019), arXiv:1904.02821 [astro-ph.HE].
 - [21] M. Mapelli, M. Spera, E. Montanari, M. Limongi, A. Chieffi, N. Giacobbo, A. Bressan, and Y. Bouffanais, ApJ **888**, 76 (2020), arXiv:1909.01371 [astro-ph.HE].
 - [22] D. Croon, S. D. McDermott, and J. Sakstein, arXiv e-prints, arXiv:2007.07889 (2020), arXiv:2007.07889 [gr-qc].
 - [23] J. Sakstein, D. Croon, S. D. McDermott, M. C. Straight, and E. J. Baxter, arXiv e-prints, arXiv:2009.01213 (2020), arXiv:2009.01213 [gr-qc].
 - [24] P. Marchant, N. Langer, P. Podsiadlowski, T. M. Tauris, and T. J. Moriya, A&A **588**, A50 (2016), arXiv:1601.03718 [astro-ph.SR].
 - [25] A. Mangiagli, M. Bonetti, A. Sesana, and M. Colpi, ApJL **883**, L27 (2019), arXiv:1907.12562 [astro-ph.HE].
 - [26] M. Fishbach and D. E. Holz, ApJL **851**, L25 (2017), arXiv:1709.08584 [astro-ph.HE].
 - [27] B. P. Abbott *et al.*, ApJL **882**, L24 (2019), arXiv:1811.12940 [astro-ph.HE].
 - [28] J. Roulet, T. Venumadhav, B. Zackay, L. Dai, and M. Zaldarriaga, arXiv e-prints, arXiv:2008.07014 (2020), arXiv:2008.07014 [astro-ph.HE].
 - [29] B. P. Abbott *et al.*, Physical Review X **9**, 031040 (2019), arXiv:1811.12907 [astro-ph.HE].
 - [30] B. Abbott *et al.*, Physical Review D **100** (2019), 10.1103/physrevd.100.064064.
 - [31] K. Chandra, V. Gayathri, J. C. Bustillo, and A. Pai, Phys. Rev. D **102**, 044035 (2020).
 - [32] J. M. Ezquiaga and D. E. Holz, arXiv e-prints, arXiv:2006.02211 (2020), arXiv:2006.02211 [astro-ph.HE].

- [33] M. C. Miller and D. P. Hamilton, *MNRAS* **330**, 232 (2002), arXiv:astro-ph/0106188 [astro-ph].
- [34] R. M. O’Leary, F. A. Rasio, J. M. Fregeau, N. Ivanova, and R. O’Shaughnessy, *ApJ* **637**, 937 (2006), arXiv:astro-ph/0508224 [astro-ph].
- [35] F. Antonini and F. A. Rasio, *ApJ* **831**, 187 (2016), arXiv:1606.04889 [astro-ph.HE].
- [36] C. L. Rodriguez, P. Amaro-Seoane, S. Chatterjee, and F. A. Rasio, *PhRvL* **120**, 151101 (2018), arXiv:1712.04937 [astro-ph.HE].
- [37] B. McKernan, K. E. S. Ford, W. Lyra, and H. B. Perets, *MNRAS* **425**, 460 (2012), arXiv:1206.2309 [astro-ph.GA].
- [38] I. Bartos, B. Kocsis, Z. Haiman, and S. Márka, *ApJ* **835**, 165 (2017), arXiv:1602.03831 [astro-ph.HE].
- [39] B. Carr, S. Clesse, J. Garcia-Bellido, and F. Kuhnel, “Cosmic conundra explained by thermal history and primordial black holes,” (2019), arXiv:1906.08217 [astro-ph.CO].
- [40] U. N. Di Carlo, N. Giacobbo, M. Mapelli, M. Pasquato, M. Spera, L. Wang, and F. Haardt, *MNRAS* **487**, 2947 (2019), arXiv:1901.00863 [astro-ph.HE].
- [41] U. N. Di Carlo, M. Mapelli, Y. Bouffanais, N. Giacobbo, F. Santoliquido, A. r. Bressan, M. Spera, and F. Haardt, *MNRAS* **497**, 1043 (2020), arXiv:1911.01434 [astro-ph.HE].
- [42] C. L. Rodriguez, M. Zevin, P. Amaro-Seoane, S. Chatterjee, K. Kremer, F. A. Rasio, and C. S. Ye, *PhRvD* **100**, 043027 (2019), arXiv:1906.10260 [astro-ph.HE].
- [43] C. L. Rodriguez, M. Zevin, P. Amaro-Seoane, S. Chatterjee, K. Kremer, F. A. Rasio, and C. S. Ye, *Physical Review D* **100** (2019), 10.1103/physrevd.100.043027.
- [44] Y. Yang, I. Bartos, V. Gayathri, K. E. S. Ford, Z. Haiman, S. Klimentenko, B. Kocsis, S. Márka, Z. Márka, B. McKernan, and R. O’Shaughnessy, *PhRvL* **123**, 181101 (2019), arXiv:1906.09281 [astro-ph.HE].
- [45] C. Kimball, C. Talbot, C. P. L. Berry, M. Carney, M. Zevin, E. Thrane, and V. Kalogera, arXiv e-prints, arXiv:2005.00023 (2020), arXiv:2005.00023 [astro-ph.HE].
- [46] V. Varma, S. E. Field, M. A. Scheel, J. Blackman, D. Gerosa, L. C. Stein, L. E. Kidder, and H. P. Pfeiffer, *Physical Review Research* **1**, 033015 (2019), arXiv:1905.09300 [gr-qc].
- [47] L. Blanchet, T. Damour, B. R. Iyer, C. M. Will, and A. G. Wiseman, *PhRvL* **74**, 3515 (1995), arXiv:gr-qc/9501027 [gr-qc].
- [48] L. Blanchet, T. Damour, G. Esposito-Farèse, and B. R. Iyer, *PhRvD* **71**, 124004 (2005), arXiv:gr-qc/0503044 [gr-qc].
- [49] T. Damour, P. Jaranowski, and G. Schäfer, *Physics Letters B* **513**, 147 (2001), arXiv:gr-qc/0105038 [gr-qc].
- [50] K. G. Arun, A. Buonanno, G. Faye, and E. Ochsner, *PhRvD* **79**, 104023 (2009), arXiv:0810.5336 [gr-qc].
- [51] L. Blanchet, *Living Reviews in Relativity* **17**, 2 (2014), arXiv:1310.1528 [gr-qc].
- [52] S. Khan, F. Ohme, K. Chatziioannou, and M. Hannam, *PhRvD* **101**, 024056 (2020), arXiv:1911.06050 [gr-qc].
- [53] A. Buonanno and T. Damour, *PhRvD* **59**, 084006 (1999), arXiv:gr-qc/9811091 [gr-qc].
- [54] A. Buonanno and T. Damour, *PhRvD* **62**, 064015 (2000), arXiv:gr-qc/0001013 [gr-qc].
- [55] S. Ossokine, A. Buonanno, S. Marsat, R. Cotesta, S. Babak, T. Dietrich, R. Haas, I. Hinder, H. P. Pfeiffer, M. Pürrer, C. J. Woodford, M. Boyle, L. E. Kidder, M. A. Scheel, and B. Szilágyi, arXiv e-prints, arXiv:2004.09442 (2020), arXiv:2004.09442 [gr-qc].
- [56] I. Mandel, *PhRvD* **81**, 084029 (2010), arXiv:0912.5531 [astro-ph.HE].
- [57] M. Fishbach, W. M. Farr, and D. E. Holz, *ApJL* **891**, L31 (2020), arXiv:1911.05882 [astro-ph.HE].
- [58] S. Galadage, C. Talbot, and E. Thrane, arXiv e-prints, arXiv:1912.09708 (2019), arXiv:1912.09708 [astro-ph.HE].
- [59] S. Miller, T. A. Callister, and W. M. Farr, *ApJ* **895**, 128 (2020), arXiv:2001.06051 [astro-ph.HE].
- [60] Z. Doctor, D. Wysocki, R. O’Shaughnessy, D. E. Holz, and B. Farr, *ApJ* **893**, 35 (2020), arXiv:1911.04424 [astro-ph.HE].
- [61] M. Fishbach, D. E. Holz, and B. Farr, *ApJL* **840**, L24 (2017), arXiv:1703.06869 [astro-ph.HE].
- [62] D. Gerosa and E. Berti, *PhRvD* **95**, 124046 (2017), arXiv:1703.06223 [gr-qc].
- [63] M. Fishbach and D. E. Holz, *ApJL* **891**, L27 (2020), arXiv:1905.12669 [astro-ph.HE].
- [64] J. Roulet and M. Zaldarriaga, *MNRAS* **484**, 4216 (2019), arXiv:1806.10610 [astro-ph.HE].
- [65] R. Abbott *et al.* (LIGO Scientific Collaboration and Virgo Collaboration), *Phys. Rev. D* **102**, 043015 (2020).
- [66] C. L. Rodriguez, M. Zevin, C. Pankow, V. Kalogera, and F. A. Rasio, *ApJ* **832**, L2 (2016).
- [67] W. M. Farr, S. Stevenson, M. Coleman Miller, I. Mandel, B. Farr, and A. Vecchio, *Nature* **548**, 426 (2017), arXiv:1706.01385 [astro-ph.HE].
- [68] S. Vitale, R. Lynch, R. Sturani, and P. Graff, *CQGra* **34**, 03LT01 (2017), arXiv:1503.04307 [gr-qc].
- [69] B. Farr, D. E. Holz, and W. M. Farr, *ApJL* **854**, L9 (2018), arXiv:1709.07896 [astro-ph.HE].
- [70] R. Essick and P. Landry, “Discriminating between neutron stars and black holes with imperfect knowledge of the maximum neutron star mass,” (2020), arXiv:2007.01372 [astro-ph.HE].
- [71] I. Mandel, W. M. Farr, and J. R. Gair, *MNRAS* **486**, 10861093 (2019).
- [72] E. Thrane and C. Talbot, *PASA* **36** (2019), 10.1017/pasa.2019.2.
- [73] S. Vitale, “One, no one, and one hundred thousand – inferring the properties of a population in presence of selection effects,” (2020), arXiv:2007.05579 [astro-ph.IM].

Appendix: Bayes factors between prior choices

In this Appendix, we compare the various mass priors considered in the main text by computing their Bayes factors given the GW190521 data. We stress that it is the goal of a hierarchical Bayesian population analysis to find the common prior that best matches a collection of data (for example, a catalog of BBH events). Here, in comparing different mass priors, we perform a population analysis on only one event; see, for example, the discussion in Ref. [70]. The goal of this Appendix is not to find the mass distribution that best fits the data, which would require analyzing multiple BBH events simultaneously, but to get a sense of how reasonable a given prior choice \mathcal{H} , $p(m_1, m_2 | \mathcal{H})$ is in light of the single-event likeli-

hood, $p(d_{\text{GW190521}} | m_1, m_2)$. The Bayesian evidence for model \mathcal{H} given data d , conditioned on d being detected, is [71–73]:

$$p(d | \mathcal{H}, \text{det}) = \frac{\int p(d | m_1, m_2) p(m_1, m_2 | \mathcal{H}) dm_1 dm_2}{\int P_{\text{det}}(m_1, m_2) p(m_1, m_2 | \mathcal{H}) dm_1 dm_2}. \quad (\text{A.1})$$

The denominator of Eq. A.1 corresponds to the expected fraction of detected systems, assuming the systems are distributed according to the model \mathcal{H} . In calculating this term, we follow the semi-analytic method described in Abbott *et al.* [27] for calculating the detection probability term $P_{\text{det}}(m_1, m_2)$, approximating the detection threshold as a single-detector signal-to-noise ratio. This denominator varies by a factor of $\lesssim 5$ between the different prior models we consider.

We consider three different prior models: an uninformative, flat prior on both masses,

$$p(m_1, m_2 | \mathcal{A}, m_{\text{min}}, m_{\text{max}}) = \frac{2}{(m_{\text{max}} - m_{\text{min}})^2}, \quad (\text{A.2})$$

an O1+O2 population-informed m_2 distribution (Eq. 1), coupled with a flat m_1 prior,

$$p(m_1, m_2 | \mathcal{B}, m_{\text{max}}) = p(m_2 | d_{\text{O1+O2}}) \frac{1}{m_{\text{max}} - m_2}, \quad (\text{A.3})$$

and an O1+O2 population-informed m_2 distribution,

coupled with a flat m_1 prior restricted to $m_1 > 120 M_{\odot}$,

$$p(m_1, m_2 | \mathcal{C}, m_{\text{max}}) = p(m_2 | d_{\text{O1+O2}}) \frac{1}{m_{\text{max}} - 120 M_{\odot}}. \quad (\text{A.4})$$

Model \mathcal{C} corresponds to the “straddling” scenario. All cases restrict $m_{\text{min}} < m_2 < m_1 < m_{\text{max}}$.

We compute the evidence ratio between these prior choices for the GW190521 mass measurement. Comparing a flat, uninformative prior between $m_{\text{min}} = 5 M_{\odot}$ and $m_{\text{max}} = 200 M_{\odot}$ (\mathcal{A}) to the population-informed m_2 prior with a flat m_1 prior in the range $m_2 < m_1 < 200 M_{\odot}$ (\mathcal{B}) gives a Bayes factor of $B_{\mathcal{A}/\mathcal{B}} = 6.8$ in favor of the uninformative prior. Meanwhile, the straddling prior \mathcal{C} is favored compared to \mathcal{B} by a factor of ~ 2 ; as discussed in the main text, imposing the population-informed prior on m_2 naturally pulls the m_1 posterior to sit above the gap. The Bayes factor comparing the uninformative prior to the straddling prior is $B_{\mathcal{A}/\mathcal{C}} = 3.4$ in favor of the uninformative prior. These near-unity Bayes factors imply that the informed priors we consider in this work, which incorporate information from previous BBH observations, are reasonable alternatives to the flat, uninformative priors.

As an additional check, we compute the Bayes factor between a double-mass-gap prior, which we take here to be model \mathcal{A} but with $m_{\text{min}} = 45 M_{\odot}$ and $m_{\text{max}} = 120 M_{\odot}$, and the straddling mass prior \mathcal{C} above. We find that, although the bulk of the GW190521 likelihood lies within the double-mass-gap mass range, the likelihood (conditioned on detection) favors the double-mass-gap prior by only a factor of 15 compared to the straddling mass prior. As long as the prior odds for a double-mass-gap merger are smaller than 1/15 (most theories predict prior odds smaller than 1/1000), the posterior odds will favor that GW190521 is a straddling binary.